EPE Journal
European Power Electronics and Drives

ISSN: 0939-8368 (Print) 2376-9319 (Online) Journal homepage: http://www.tandfonline.com/loi/tepe20

Generalized Algorithm for Pulse Width Modulation Using a Two-Vectors Based Technique

José Restrepo, José M. Aller, Alexander Bueno, Víctor M. Guzmán & María I. Giménez

To cite this article: José Restrepo, José M. Aller, Alexander Bueno, Víctor M. Guzmán & María I. Giménez (2011) Generalized Algorithm for Pulse Width Modulation Using a Two-Vectors Based Technique, EPE Journal, 21:2, 30-39, DOI: 10.1080/09398368.2011.11463793

To link to this article: http://dx.doi.org/10.1080/09398368.2011.11463793

José Restrepo, José M. Aller, Alexander Bueno, Víctor M. Guzmán, María I. Giménez, Universidad Simón Bolívar

Generalized Algorithm for Pulse Width Modulation using a Two-Vectors Based Technique

José Restrepo, José M. Aller, Alexander Bueno, Víctor M. Guzmán, María I. Giménez, Universidad Simón Bolívar, Valle de Sartenejas, Baruta, Edo. Miranda, Caracas, Venezuela

Keywords: Space vector modulation, Vector coordinates, Natural coordinates, Null vector ratio, Parallelogram, PWM, Inverter, DC-AC power conversion

Abstract

This paper presents a generalized and compact space vector modulation algorithm valid for both (a, b, c) and (x, y) coordinates, suitable for triangle comparison modulators. The proposed algorithm uses a two base-vectors duty cycle computation by mapping the solution space into only three parallelogram shaped zones (Fig. A). This generalized algorithm is especially suited for vector control applications requiring high dynamic response and for applications where changes in demand may happen at a frequency comparable with the modulator's carrier frequency. Several carrier base modulation methods extensively described in the literature are obtained from the proposed generalized space vector modulation algorithm with the introduction of the null vector ratio δ. The proposed method has been experimentally tested, and a practical implementation of the generalized algorithm with low computational requirements is presented.

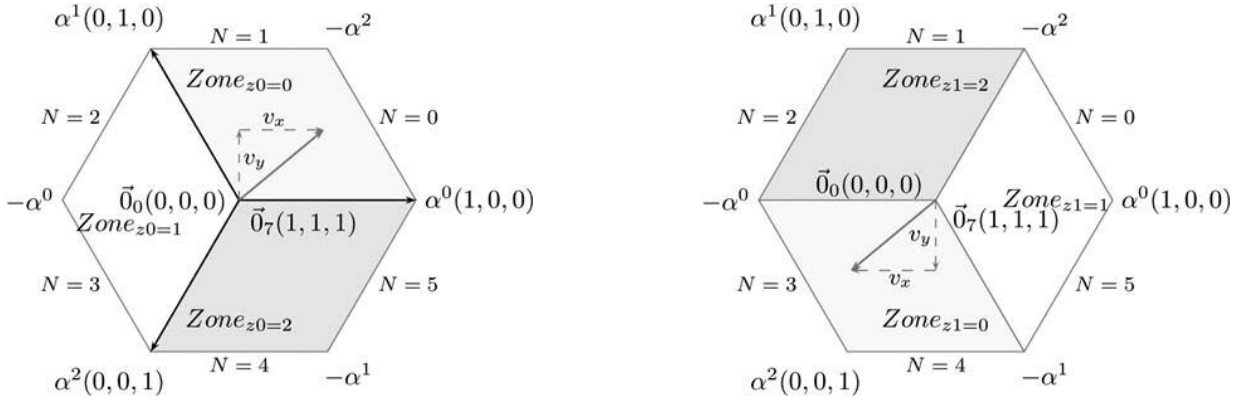

(a) Zones for $D_{0,z0+2} = 0$ (b) Zones for $D_{1,z1+2} = 0$

Fig. A: Normalized averaged inverter's output mapped in the hexagonal space

Introduction

The standard voltage source inverter (VSI) shown in Fig. 1 can be found in many modern applications, as part of complex topologies such as the dual converter [1], multiphase configurations [2, 3], induction motor drive applications [4, 5], or in general applications requiring precise control of power flow from AC to DC or vice versa [6]. Much research have been devoted towards the development of efficient ways for controlling this type of converters with a low computational burden in its implementation [7, 8], or attaining low common mode voltages [9], low harmonic contamination [10, 11], reduced switching losses [12], low electromagnetic interference [13] and flexibility in the selection of the modulation strategy while using standard control hardware [14]. From the techniques used in the control of power converters such as delta modulation, selective harmonic elimination, hybrid pulse width modulation (hybrid-PWM) techniques, among others [10], carrier based PWM [15] has been in general the preferred choice, and over the past decades several variants of this technique have been studied [16, 17, 18, 19]. With the availability of a constantly increasing processing power, high performance control strategies based on space vector theory become possible, and Space Vector Pulse Width Modulation (SVPWM) [20] seems especially suited for these and similar high dynamic control schemes, hence SVPWM has also been a subject of extensive research, in [21] a generalized discontinuous PWM scheme is proposed. Also, optimal algorithms for the implementation of general SVPWM have been presented in [7, 8, 22, 23].

This work proposes an algorithm specially suited for applications requiring frequent changes in modulation strategies, such as the one presented in [6] or, in general, for the generation of a per carrier period average voltage space vector. The main contributions made in this paper can be summarized as follows

– Development of a unifying algorithm for implementing all the modulation strategies with central symmetry pulses, that can be indistinctly applied to systems described either in natural coordinates or using space vectors in coordinates.
– Definition of a sector identification expression that uses only the sign function, logic comparisons and the arithmetic operations addition, subtraction and multiplication.
– Application of the algorithm to continuous or discontinuous modulation such as SVPWM, $DPWM_{min}$, $DPWM_{max}$,

$DPWM_{(0,1,2,3)}$, [7, 16, 21] through the use of closed form formulas employing a single parameter for implementing the desired modulation strategy.
– Generation of the duty cycle for each converter's branch required for synthesizing an average space vector $\vec{v}$, using standard PWM circuitry with a reduced number of operations, suitable for implementation with low end micro-controllers.

As pointed out previously, the proposed algorithm uses two base-vectors defining three parallelogram shaped sectors or zones, covering the hexagonal space produced by the converter shown in Fig. 1. The use of one clamped converter branch helps to visualize the synthesis of the space vector with the switching of the remaining branches (two base-vectors modulation technique).

Seven experimental examples using the proposed technique have been tested in the laboratory and the results show the advantages of using a generalized algorithm in its own coordinates system.

The proposed algorithm has been applied successfully to a dual converter employed as a rectifier with power factor regulation and bidirectional power flow [24].

Generalized space vector modulation

The typical three phase converter shown in Fig. 1 has $4^3 = 64$ possible states, of which $3^3 = 27$ are allowed (those that do not short circuit the DC link) and only $2^3 = 8$ states have a single power device turned "on" in each branch. Three of these states can be considered a base to produce the remaining five states, vectors (α^0, α^1, α^2), corresponding to states (1, 0, 0), (0, 1, 0) and (0, 0, 1) respectively. In this representation a "1" corresponds to an upper power device turned "on" in the inverter branch, while the lower device is turned "off", and a "0" corresponds to a lower power device turned "on" while the upper device is turned "off" in the inverter branch.

Any average voltage space vector can be obtained by using Clarke's transformation:

$$\vec{v} = \xi\left(v_{aN}\alpha^0 + v_{bN}\alpha^1 + v_{cN}\alpha^2\right) \tag{1}$$

ξ usually takes the values 1, 2/3 or $\sqrt{2}/3$. Normalizing by ξV_{DC}, the per unit vector is,

$$\begin{aligned}\vec{v}_{pu} &= v_x + jv_y = \frac{1}{V_{DC}}\left(v_{aN}\alpha^0 + v_{bN}\alpha^1 + v_{cN}\alpha^2\right) = \\ &= \frac{1}{V_{DC}}\left[\left(v_a - v_N\right) + \left(v_b - v_N\right)\alpha + \left(v_c - v_N\right)\alpha^2\right] = \\ &= \left(D_a + D_b\alpha + D_c\alpha^2\right)\end{aligned} \tag{2}$$

where v_{aN}, v_{bN} and v_{cN} are the phase voltages with respect to the DC supply's negative rail, as shown in Fig. 1, $\alpha = e^{j2\pi/3}$, and D_a, D_b, D_c are the duty cycles for each inverter branch.

The instantaneous space vector's magnitude in the VSI depends on the value of ξ, and it is found to be $|v_{a\_max}\alpha^0| = |v_{b\_max}\alpha^1| = |v_{c\_max}\alpha^2| = \xi V_{DC}$. However, with the use of pulse width modulation each branch's average voltage can be controlled during a carrier signal's period.

This paper proposes a general and compact SVPWM algorithm for synthesizing any space vector, in the normalized hexagonal space covered by the base vectors. The method uses a two base-vectors technique suitable for triangle intersection modulators, also known as carrier based modulators. This generalized method can be applied to systems described in natural coordinates (*a, b, c*) or in systems described using space vectors (*x, y*); to achieve this, compact expressions for sector selection using only basic mathematical operations are introduced. However, there are other switching strategies, such as type III and type IV sequences [25], or special sequences for ripple minimization that are not suitable for standard triangular carrier implementations [10, 26] and therefore are not covered by the proposed generalized algorithm.

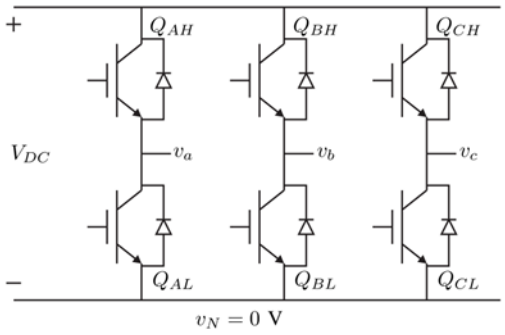

Fig. 1: Voltage source inverter (VSI) circuit diagram

The ratio of the time spent in state (0,0,0) versus the time spent in state (1,1,1), when both vectors are used to synthesize the zero vector in a particular PWM period, has been traditionally used as the base for different generalized SVPWM algorithms [14, 16] [27, 28, 29]. This ratio will be referred in this work as the null vector ratio δ, and will be used both for natural coordinates and for space vector description. In general δ can take any value between zero and one and, at the same time, this value can be altered from control period to control period, depending on the modulation strategy. For $\delta = 1$, the zero vector is synthesized by using only state (0,0,0), similarly for $\delta = 0$, the zero vector is synthesized by using only state (1,1,1).

Generalized space vector modulation in (*x, y*) coordinates

Modern control strategies are usually described using a two coordinates representation of electric space state variables such as voltage, current, flux, etc. For three phase systems, this space vector description has the advantage of reducing the number of equations required for a dynamical modeling of the system under control. Although the duty cycles required by the physical VSI can be readily obtained by using a two-phase to three-phase transformation of the demanded voltages, a direct procedure based on the modulation of two active branches is proposed in this work.

Basic underlying method: The core idea of the proposed method is based on synthesizing, in an averaged sense, any normalized space vector $\vec{v}_{pu} = v_x + jv_y$ by adjusting the "on" time of the two neighboring base vectors (α^0 and α^1, α^1 and α^2, or α^2 and α^0) during the switching period of the modulator. Fig. 2 shows the synthesis of a space vector falling inside the area covered by the base vectors (α^0, α^1) and the decomposition of the space vector in fractions of the corresponding base vectors [30]. Fig. 2a corresponds to a synthesis of the null vector using state (0,0,0) and Fig. 2b to the synthesis of the null vector using state (1,1,1).

For the decomposition shown in Fig. 2a, one of the phases is always "off", so, the synthesis of space vector $\vec{v}_{pu}$ is done by applying the base vectors α^0 and α^1 for lengths of time equivalent

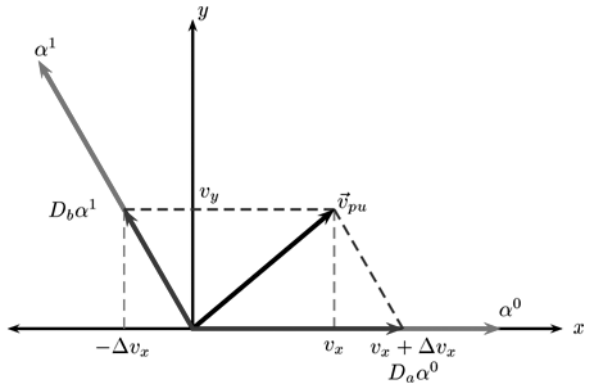

(a) Null vector using (0,0,0)

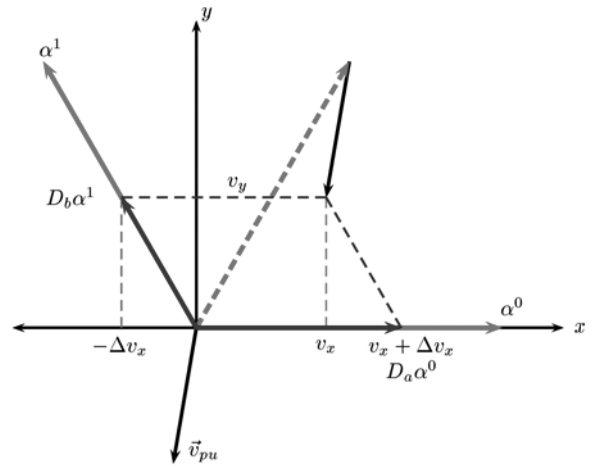

(b) Null vector using (1,1,1)

Fig. 2: Space vector decomposition as fraction of neighboring base vectors for the cases where the null vector is synthesized with (0,0,0) shown in (a) or (1,1,1) shown in (b).

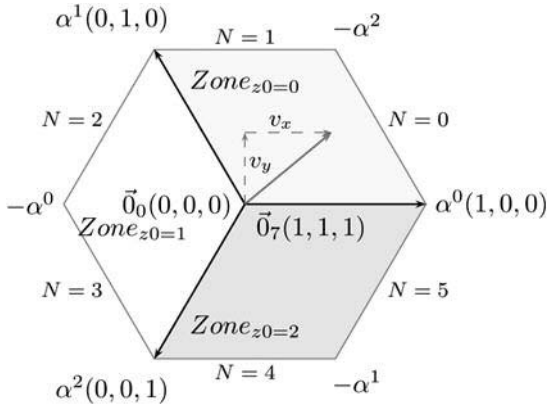

(a) Parallelogram zones for $z0$ ($D_{0,z0+2} = 0$)

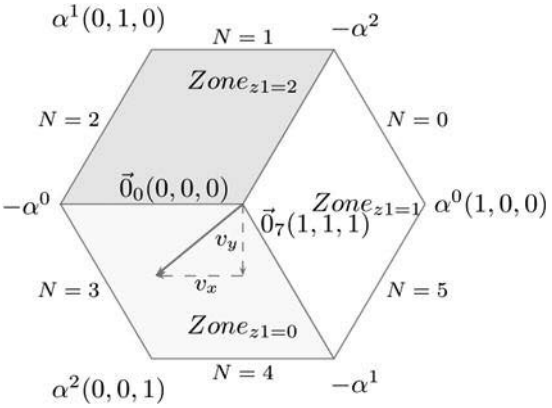

(b) Parallelogram zones for $z1$ ($D_{1,z1+2} = 1$)

Fig. 3: Normalized inverter's output mapped in the hexagonal space

to D_aT_s and D_bT_s respectively, while the branch associated with the base vector α^2 is always "off" (i.e. in low level). T_s is the modulator's carrier switching period. From Fig. 2a, the projections of the space vector $\vec{v}_{pu}$ into base vectors α^0 and α^1 (D_a,D_b) are:

$$D_a = v_x + \Delta v_x = v_x - D_b \cos\left(\frac{2\pi}{3}\right) = v_x - v_y \cot\left(\frac{2\pi}{3}\right) = v_x + \frac{v_y}{\sqrt{3}}$$

$$D_b = \frac{v_y}{\sin\left(\frac{2\pi}{3}\right)} = \frac{2v_y}{\sqrt{3}} \tag{3}$$

The proposed procedure can be explained as follows:

Definition of terms and parallelogram zones: The null vector can be obtained using only state $\vec{0}_0$ = (0, 0, 0) or state $\vec{0}_7$ = (1, 1, 1). When the null vector is synthesized using only state $\vec{0}_0$, the hexagonal space is divided in three parallelogram zones $z0 = \{0,1, 2\}$ as shown in Fig. 3(a). In this case, the space vector is synthesized with the non-switching branch in state "0". Otherwise, when the synthesis of the null vector is done solely with state $\vec{0}_7$, the hexagonal space is divided in the three parallelogram shaped zones $z1 = \{0,1, 2\}$ shown in Fig. 3(b), and the space vector is synthesized with the non-switching branch in state "1". The two three-parallelogram sets are represented as zn, where $n = \{0, 1\}$, for operation in $z0$ or $z1$. Each parallelogram is bounded by two vectors. In $z0$ the vectors are (α^{z0}, α^{z0+1}) and in $z1$ the vectors are ($-\alpha^{z1}$, $-\alpha^{z1+1}$), where $\alpha = e^{j2\pi/3}$. Each parallelogram can be identified by the vector α^{z0} (Fig. 3(a)) or $-\alpha^{z1}$ (Fig. 3(b)), which are respectively the first base vectors in the boundary of the corresponding parallelogram zone for a space vector $\vec{v}_{pu}$ moving anticlockwise. The general zone, zn = {0,1, 2}, can be rotated to the base parallelogram ($zone_{z0=0}$) defined by vectors α^0 and α^1

As shown in Fig. 3, the non-switching branch's state $D_{n,zn+2} = n$ defines the operation for $n = 0$ (Fig. 3(a)) and for $n = 1$ (Fig. 3(b)). The algorithm for the synthesis of space vectors using both descriptions shown in Fig. 3 can be simplified with the use of a sector identifier N ∈ {0, …, 5}, obtained from the space vector's angle θ using,

$$N = \left\lfloor \frac{3\theta}{\pi} \right\rfloor, \qquad \theta = \arctan\left(\frac{v_y}{v_x}\right) \tag{4}$$

where $[x] = \max\{n \in \mathbb{Z} \mid n \le x\}$ = floor (x). Zones $z0$ and $z1$ are defined using the sector identifier N with the following expressions,

$$z0 = \left\lfloor \frac{N}{2} \right\rfloor, \qquad z1 = \left\lfloor \frac{N+3}{2} \right\rfloor \tag{5}$$

$z0$ and $z1$ are modulo 3 integers.

Duty cycles for the generalized zone: From (2) the normalized space vector $\vec{v}_{pu}$ can be written using the following notation:

$$\vec{v}_{pu} = D_0\alpha^0 + D_1\alpha^1 + D_2\alpha^2 \quad (6)$$

Using a more general notation, (6) becomes,

$$\vec{v}_{pu} = D_{n,zn}\alpha^{zn} + D_{n,zn+1}\alpha^{zn+1} + D_{n,zn+2}\alpha^{zn+2} \quad (7)$$

The two vectors decomposition shown in Fig. 2 can be obtained from (7) by enforcing two restrictions. First, one of the branches is not switching, *zn* is selected so that branch *zn* + 2 is the non-switching branch, this means that $D_{n,zn+2}$ can take the values {0, 1}. The second restriction forces the duty cycle of the switching branches $\{D_{n,zn}, D_{n,zn+1}\}$ to be in the range [0⟷1]. The decomposition described by (3), corresponding to *zn* = 0, can be generalized to any zone *zn* by re-writing (7) as

$$\left(\vec{v}_{pu} - \alpha^{zn+2}D_{n,zn+2}\right)\alpha^{-zn} = \alpha^0 D_{n,zn} + \alpha^1 D_{n,zn+1} \quad (8)$$

This means that zone *z*0 = 0, bounded by vectors α^0 and α^1, is used as the base parallelogram for producing the duty-cycles $D_{n,zn}$ and $D_{n,zn+1}$, required by any vector in $zone_{zn}$. The synthesis of a normalized space vector in $zone_{zn}$ using the base zone is achieved by shifting the space vector $\vec{v}_{pu}$ defined in equation (2), adding vector $-\alpha^{zn+2}D_{n,zn+2}$ (corresponding to the non-switching branch) and rotating the resulting vector an angle α^{-zn}, as shown in Fig. 4.

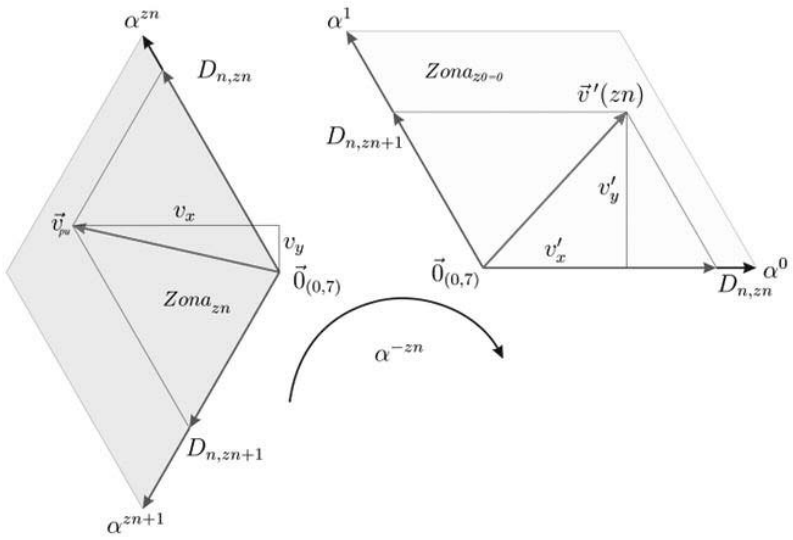

Fig. 4: Space vector synthesis using the transference from parallelogram $zone_{zn}$ to the base parallelogram $zone_{z0=0}$

Defining the normalized and rotated vector as,

$$\vec{v}'(zn) = v'_x + jv'_y = v_{pu}\alpha^{-zn} \quad (9)$$

and replacing (9) in (8),

$$\vec{v}'(zn) - \alpha^2 D_{n,zn+2} = \alpha^0 D_{n,zn} + \alpha^1 D_{n,zn+1} \quad (10)$$

Replacing in (10) the duty cycle for the non-switching branch $D_{n,zn+2} = n$, and the values for α^0, α^1 and α^2, (10) becomes,

$$v'_x + jv'_y - \left(\frac{1}{2} + j\frac{\sqrt{3}}{2}\right)n = D_{n,zn} - \left(\frac{1}{2} - j\frac{\sqrt{3}}{2}\right)D_{n,zn+1} \quad (11)$$

The resulting duty cycles are,

$$\begin{aligned} D_{n,zn} &= v'_x + \frac{v'_y}{\sqrt{3}} + n \\ D_{n,zn+1} &= \frac{2v'_y}{\sqrt{3}} + n \\ D_{n,zn+2} &= n \end{aligned} \quad (12)$$

where $D_a = D_{n,0}$, $D_b = D_{n,1}$ and $D_c = D_{n,2}$, and the sub-indexes operate using (mod 3) arithmetic.

Generalized space vector modulation in natural coordinates *(a, b, c)*

A simple SVPWM implementation in natural (*a, b, c*) coordinates using normalized phase voltages, when zero vector is synthesized using only state (0, 0, 0) [7, 16], is provided by the following expressions:

$$D_{0,p} = \left(v_{pN} - v_{min}\right) \qquad p = a, b, c. \quad (13)$$

and for zero vector synthesized using only state (1,1,1):

$$D_{1,p} = \left(1 + v_{pN} - v_{max}\right) \qquad p = a, b, c. \quad (14)$$

where the voltages are normalized by V_{DC} and,

$$v_{min} = \frac{1}{V_{DC}}\min(v_{aN}, v_{bN}, v_{cN})$$

$$v_{max} = \frac{1}{V_{DC}}\max(v_{aN}, v_{bN}, v_{cN})$$

These two possible ways to synthesize a space vector will be used afterwards in the scalar version of the generalized SVPWM algorithm.

Generalized SVPWM using the null vector ratio δ

A parameter similar to the null vector ratio δ has been traditionally proposed as a control parameter to define several modulation techniques [14, 16, 21, 28, 29]. As a simple first modulation strategy, δ provides a way to combine the resulting duty cycles obtained when the zero vector is synthesized using states (0, 0, 0) and (1, 1, 1). For a more general modulation strategy, this parameter can be a function of the space's vector angular position.

Application of null vector ratio δ for (x, y) coordinates

The duty cycles for the VSI switches in the generalized vector based algorithm are obtained by averaging the ones calculated from (12) for both possible states, *n* = {0, 1}, by using the null vector ratio δ with the following expression,

$$D_k = \delta D_{0,k} + (1-\delta)D_{1,k} \qquad k = \{0,1,2\} \quad (15)$$

Table I: Duty cycle selection using $z0$ and $z1$

z_n	$D_{n,0}$	$D_{n,1}$	$D_{n,2}$
0	$v_x + \frac{v_y}{\sqrt{3}} + n$	$\frac{2v_y}{\sqrt{3}} + n$	n
1	n	$-v_x + \frac{v_y}{\sqrt{3}} + n$	$-v_x - \frac{v_y}{\sqrt{3}} + n$
2	$v_x - \frac{v_y}{\sqrt{3}} + n$	n	$-\frac{2v_y}{\sqrt{3}} + n$

The practical implementation of the modulation algorithm is simplified by defining the following intermediate variables,

$$f_x = v_x; \qquad f_y = \frac{v_y}{\sqrt{3}}. \tag{16}$$

Using these variables, the sector identifier $N(f_x, f_y)$ is:

$$N(f_x, f_y) = \left\lfloor \frac{3\theta}{\pi} \right\rfloor = \frac{5}{2} - \mathrm{sgn}(f_y)\left[H(f_x - f_y) + H(f_x + f_y) + \frac{1}{2} \right] \tag{17}$$

Where $H(\cdot)$, the Heaviside function, commonly known as the step function, is zero for a negative argument and one otherwise.

$N(f_x, f_y)$ locates the space vector to be synthesized in one of the zones in the hexagonal space, and defines the expressions needed for computing the required duty cycles D_a, D_b and D_c, presented in Table II. This sector identifier is obtained using only magnitude comparisons and simple arithmetic operations such as additions and multiplications.

Table II is filled row by row using the following procedure:

– First, the sector identifier N is obtained from (4) to determine $z0$ and $z1$;
– Sub-index zn in (12) is replaced, as indicated in Table I, to obtain the resulting duty cycles;
– The final expression for D_k is obtained as a function of δ, f_x and f_y by applying (15);
– Select the null vector ratio δ for the desired modulation.

For example, the entry corresponding to $N = 3$ is obtained as follows,

– For $N = 3$, $z0 = 1$ and $z1 = 0$;
– The duty cycles are selected from Table I, according to $z0$ and $z1$,

$z0 = 1$	$z1 = 0$
$D_{0,0} = 0$	$D_{1,0} = v_x + \frac{v_y}{\sqrt{3}} + 1 = f_x + f_y + 1$
$D_{0,1} = -v_x + \frac{v_y}{\sqrt{3}} = -f_x + f_y$	$D_{1,1} = \frac{2v_y}{\sqrt{3}} + 1 = 2f_y + 1$
$D_{0,2} = -v_x - \frac{v_y}{\sqrt{3}} = -f_x - f_y$	$D_{1,2} = 1$

– The final duty cycles as a function of δ, f_x and f_y are obtained using (15),

$$D_a = D_0 = \delta(0) + (1-\delta)(f_x + f_y + 1) = D_c + f_x + f_y$$

$$D_b = D_1 = \delta(-f_x + f_y) + (1-\delta)(2f_y + 1) = D_c + 2f_y$$

$$D_c = D_2 = \delta(-f_x - f_y) + (1-\delta)(1) = \delta(-f_x - f_y - 1) + 1$$

Table II can be used directly for implementing the generalized SVPWM as a function of the null vector ratio δ.

Application of null vector ratio δ for natural coordinates

For natural coordinates, the duty cycles for the VSI switches in the generalized vector based algorithm are obtained using (15). In this case, the duty cycles $D_{0,p}$ and $D_{1,p}$ are given by (13) and (14), and the averaged duty cycles are:

$$D_p = (1-\delta)(1 - v_{max}) - \delta v_{min} + v_{pN} \qquad \{p = a, b, c\} \tag{18}$$

Since in natural coordinates the different modulation strategies are obtained by zero sequence component injection [19, 28, 31], the zero sequence voltage required by the selected modulation strategy is,

$$v_0 = (1-\delta)(1 - v_{max}) - \delta v_{min} \tag{19}$$

and the duty cycles are,

$$D_p = v_0 + v_p \qquad \{p = a, b, c\} \tag{20}$$

The classical SVPWM can be obtained by selecting $\delta = 1/2$

Generalized modulation methods using δ

As mentioned in the introduction, the number of modulation methods is in theory infinite, depending on the choice of the null vector ratio δ, but only a few have been reported to be of practical use [30, 32]. The modulation methods can be divided in continuous PWM (CPWM) and discontinuous PWM (DPWM) in natural or (x, y) coordinates. The general method proposed in this work reproduces the modulation strategies SVPWM, $DPWM_0$, $DPWM_1$, $DPWM_2$ and $DPWM_3$ presented in [16]. This is done by setting the null vector ratio δ depending on the angle θ of the demanded inverter space voltage vector $\vec{v}_{pu} = v_x + jv_y$. Table III presents the δ value for each modulation strategy.

Although the generalized algorithm is the linear combination of two discontinuous modulation methods ($DPWM_{min}$ and $DPWM_{max}$), the standard sinusoidal modulation can be represented

Table II: Expressions for duty cycles required in the practical implementation of the generalized algorithm

N	$z0$	$z1$	D_a	D_b	D_c
0	0	1	$\delta(f_x + f_y - 1) + 1$	$D_a - f_x + f_y$	$D_a - f_x - f_y$
1	0	2	$D_b + f_x - f_y$	$\delta(2f_y - 1) + 1$	$D_b - 2f_y$
2	1	2	$D_b + f_x - f_y$	$\delta(-f_x + f_y - 1) + 1$	$D_b - 2f_y$
3	1	0	$D_c + f_x + f_y$	$D_c + 2f_y$	$\delta(-f_x + f_y - 1) + 1$
4	2	0	$D_c + f_x + f_y$	$D_c + 2f_y$	$\delta(-2f_y - 1) + 1$
5	2	1	$\delta(f_x - f_y - 1) + 1$	$D_a - f_x + f_y$	$D_a - f_x - f_y$

by adjusting δ as a function of the space vector's angle θ. As an example, if a sinusoidal signal of maximum amplitude is to be synthesized in each branch, this has to be centered around $V_{DC}/2$, resulting for a three phases system in a constant zero sequence modulation strategy. In this example, the duty cycles are,

$$\begin{aligned} D_a(t) &= \frac{1}{2}\left[1+\sin(\omega t+\phi)\right] \\ D_b(t) &= \frac{1}{2}\left[1+\sin(\omega t+\phi-2\pi/3)\right] \\ D_c(t) &= \frac{1}{2}\left[1+\sin(\omega t+\phi-4\pi/3)\right] \end{aligned} \tag{21}$$

resulting in,

$$D_a(t) + D_b(t) + D_c(t) = \frac{3}{2} \tag{22}$$

Replacing (22) in (15), the null vector ratio δ results in,

$$\delta = \frac{\frac{3}{2} - \sum D_{1,k}}{\sum (D_{0,k} - D_{1,k})} \qquad \{k = 0,1,2\} \tag{23}$$

For a vector voltage's angle in the range $0 < \theta < \pi/3 \rightarrow N = 0$, and replacing the duty cycles from (12), the resulting null vector ratio δ is:

$$\delta = \left[\frac{\frac{2}{3}v_x - \frac{1}{2}}{v_x + \frac{v_y}{\sqrt{3}} - 1} \right] \tag{24}$$

If the space's vector angle θ is outside the range [0, π/3], $\vec{v}_{pu}$ can be rotated

$$\alpha^{-\frac{\pi}{3}N}$$

to be represented by (24),

$$\vec{v}_r = v_{rx} + jv_{ry} = (v_x + jv_y)\cdot\alpha^{-\frac{\pi}{3}N} \tag{25}$$

Finally, the description of SVPWM with the generalized algorithm for any vector $\vec{v}_{pu} = v_x + jv_y$, can be obtained using the following value for δ,

$$\delta = \left[\frac{\frac{2}{3}v_{rx} - \frac{1}{2}}{v_{rx} + \frac{v_{ry}}{\sqrt{3}} - 1} - \frac{1}{2} \right](-1)^N + \frac{1}{2} \tag{26}$$

This expression for the null vector ratio can also be obtained directly from natural coordinates using (19),

$$\delta = \frac{\frac{1}{2} - v_{max}}{1 - v_{max} + v_{min}} \tag{27}$$

Since the null vector ratio δ can be described either in (x, y) coordinates using (26) or in natural coordinates (a, b, c) using (27), the computational burden of coordinates transformation is eliminated.

Table III: δ value for some common modulation strategies using the proposed Generalized Algorithm [24]

Modulation	δ
$DPWM_{min}$	1
$DPWM_{max}$	0
SVPWM	1/2
$DPWM_0$	$\frac{1}{2}\left[1+(-1)^{n_1}\right]$
$DPWM_1$	$\frac{1}{2}\left[1+(-1)^{n_2}\right]$
$DPWM_2$	$\frac{1}{2}\left[1+(-1)^{(n_1+1)}\right]$
$DPWM_3$	$\frac{1}{2}\left[1+(-1)^{(n_2+1)}\right]$
SPWM	$\left[\frac{\frac{2}{3}v_{rx}-\frac{1}{2}}{v_{rx}+\frac{v_{ry}}{\sqrt{3}}-1}-\frac{1}{2}\right](-1)^{n_1}+\frac{1}{2}$ $v_{rx}+jv_{ry}=(v_x+jv_y)\cdot\alpha^{-\frac{\pi}{3}n_1}$
For (x, y) coordinates: $n_1 = N = 2.5 - sign(f_y)\left[H(f_x - f_y) + H(f_x + f_y) + 0.5\right]$ $n_2 = 3.5 - sign(f_x + 3f_y)\left[H(f_x) + H(f_x - 3f_y) + 0.5\right]$	
For (a, b, c) coordinates: $n_1 = N = 2.5 - sign(v_{bN} - v_{cN})\left[H(v_{aN} - v_{bN}) + H(v_{aN} - v_{cN}) + 0.5\right]$ $n_2 = 3.5 + sign(v_{cN})\left[H(v_{aN}) + H(v_{aN} + v_{cN}) + 0.5\right]$	

Experimental results

In the practical implementation of any algorithm there are several factors that need to be considered to optimize the code length and complexity of the operations used. For low end processors, no transcendental functions should be employed, and the number of operations must be kept to a minimum. To achieve this with the proposed generalized algorithm, the intermediate variables

defined in (16) are used for operation in (x, y) coordinates.

The superposition of the parallelogram zones in the hexagonal space shown in Fig. 3 results in the traditional six triangular sectors. Table II presents the duty cycles corresponding to each sector identifier N in the hexagon, as a function of the null vector ratio δ. This table is a direct representation of the practical implementation of the generalized algorithm.

For the algorithm practical implementation, computation of the null vector ratio δ in Table III for $DPWM_0$, $DPWM_1$, $DPWM_2$ and $DPWM_3$ is simplified by extracting the least significant bit (LSB) of n_1 or n_2 as follows,

$DPWM_0 \rightarrow \quad \delta = \text{not}(n_1 \ \& \ 1)$
$DPWM_1 \rightarrow \quad \delta = \text{not}(n_2 \ \& \ 1)$
$DPWM_2 \rightarrow \quad \delta = (n_1 \ \& \ 1)$
$DPWM_3 \rightarrow \quad \delta = (n_2 \ \& \ 1)$

Table IV shows the computational burden for different modulation strategies, and Table V shows the execution time for the experimental implementation done in this work.

The proposed generalized algorithm was implemented on a custom build floating point DSP (ADSP-21061-40 MHz) based test-rig. The power stage uses six 50 A, 1200 V, IGBTs with a 2200 µF 450 V capacitor in the DC link. The load is made of three star connected inductors with L = 10.0 mH, and R = 0.05 Ω.

The PWM signals are obtained from a motion coprocessor ADMC-201AP with the following operating conditions:

Clock Frequency	8 MHz
Dead time	500 ns
Pulse deletion	500 ns
PWM master switch period selection	800

With this setup the PWM circuitry is operating at 10 kHz switching frequency, and the registers for programming the PWM duty cycles use integers in the range [0 $\longleftrightarrow$ 800] for duty cycles between 0 % and 100 %. Figs. 5 and 6 show the current and trigger signals for phase "a" when, respectively, the modulation methods $DPWM_{min}$, $DPWM_{max}$, $DPWM_0$, $DPWM_1$, $DPWM_2$ and $DPWM_3$ are applied to the power converter for a circular trajectory in the linear region with a modulation index of 0.866. Although the trigger signals for the VSI devices have different shapes, the current waveforms and their harmonics content appear the same for the six different modulation methods.

The harmonic content of the phase voltages and load currents for

Table IV: Computational burden for different SVPWM strategies

function	δ constant	$DPWM_0$	$DPWM_1$	$DPWM_2$	$DPWM_3$	
Multiplications	7	6	8	6	8	(x,y) coordinates
Sums	10	11	15	10	14	
Logic Operations	2	3	5	3	5	
sign( )	1	1	2	1	2	
Multiplications	5	6	6	6	6	(a,b,c) coordinates
Sums	6	11	10	10	9	
Logic Operations	2	2	2	2	2	
min( )	2	2	2	2	2	
max( )	0	3	3	3	3	
sign( )	0	1	1	1	1	

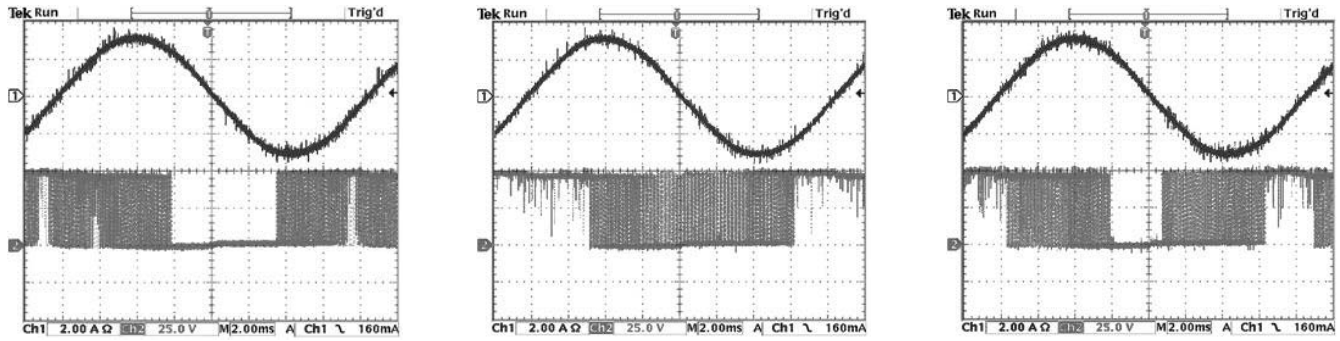

(a) $DPWM_{min}$ (b) $DPWM_{max}$ (c) $DPWM_0$

Fig. 5: Experimental phase "a" current and trigger signal for $DPWM_{min}$, $DPWM_{max}$ and $DPWM_0$ methods.

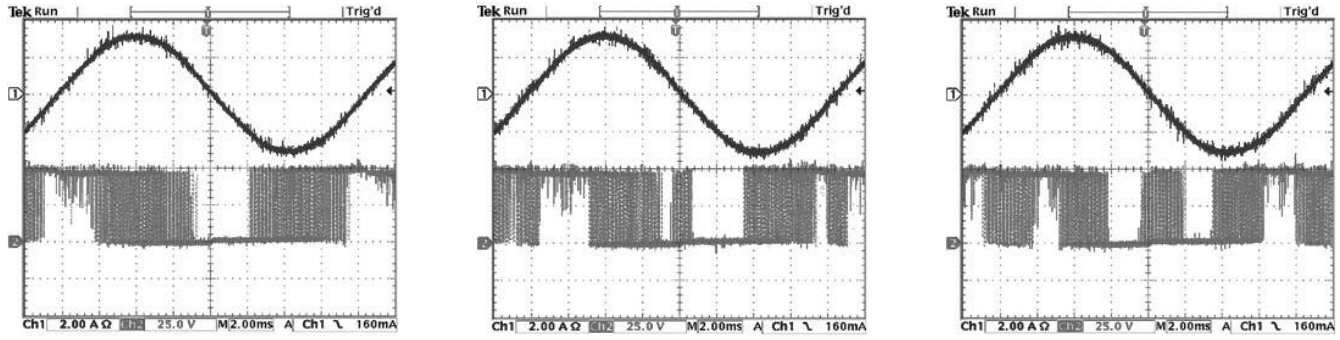

(a) $DPWM_1$ (b) $DPWM_2$ (c) $DPWM_3$

Fig. 6: Experimental phase "a" current and trigger signal for $DPWM_1$, $DPWM_2$ and $DPWM_3$ methods.

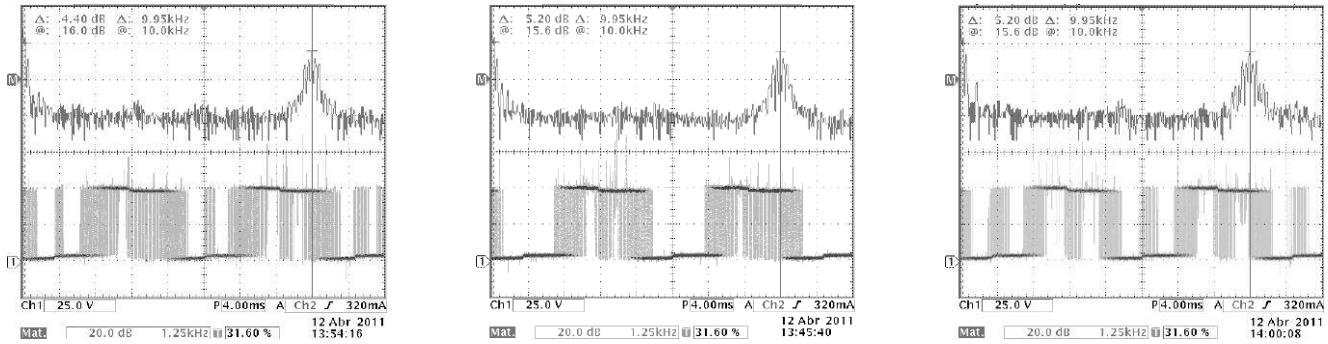

(a) Phase voltage and spectrum (SVM) (b) Phase voltage and spectrum ($DPWM^{min}$) (c) Phase voltage and spectrum ($DPWM_3$)

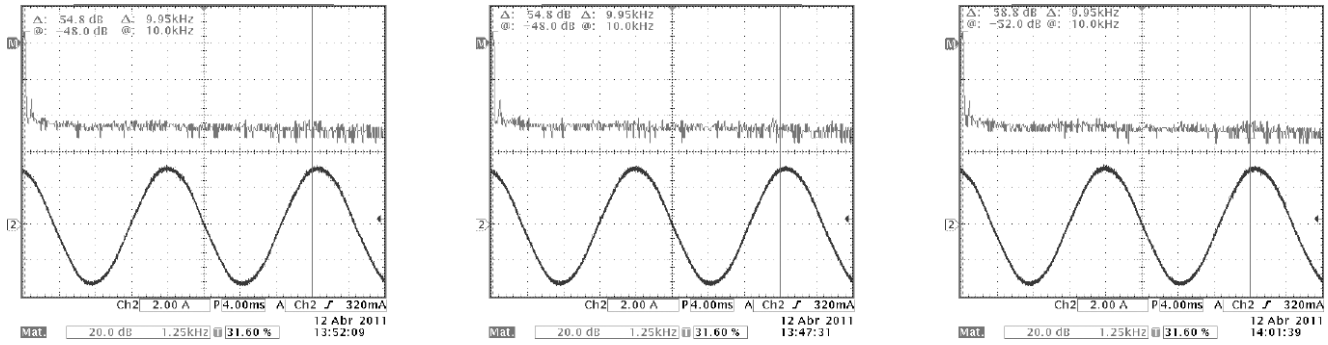

(d) Phase current and spectrum (SVM) (e) Phase current and spectrum ($DPWM^{min}$) (f) Phase current and spectrum ($DPWM_3$)

Fig. 7: Experimental phase "a" voltage and current harmonics spectrum for three modulation methods SVM, $DPWM_{min}$ and $DPWM_3$

Table V: Execution time for different SVPWM algorithms, running on a DSP-21061 at 40 MHz

Modulation Method	Time in µs	
	(x, y) coord.	(a, b, c) coord.
$DMPWM_{min}$ $DMPWM_{max}$ SVPWM	1.62	1.03
$DMPWM_0$ $DMPWM_1$	2.18	2.13
$DMPWM_2$ $DMPWM_3$	2.15	2.10

three modulation methods (SVM, $DPWM_{min}$, $DPWM_3$) are shown in Fig. 7. As mentioned before, it can be seen that the voltage waveforms are different for each modulation method, and the effect on the high frequency current harmonics is negligible. There are minor differences in the low order voltage harmonic content for the modulation methods analyzed in this work.

Conclusion

A generalized method using a two base-vectors algorithm for producing per phase duty cycles, for references in vector (x, y) and natural (a, b, c) coordinates has been proposed. The proposed generalized modulation method is especially suited for controllers requiring high dynamic response such as FOC, DTC, DPC, etc., and does not require additional coordinate transformations. This method can be used to adaptively select the most suitable modulation strategy that reduces the current stress and minimizes the inverter switching losses, by properly selecting the null vector ratio δ, depending on the current vector magnitude and position [6]. An advantage of the proposed generalized method is that it employs the triangle intersection technique and the resulting duty cycles can be readily fed to existing carrier based PWM modules. The mathematical operations required by the practical implementation of the proposed generalized algorithm are simple multiplications, additions, and logical comparisons used to reduce the number of jumps in the low level code, making it suitable for its implementation in low performance processors.

For modern control applications with high computational loads, the algorithm runs in about 2.0 µs, corresponding to 2 % of the control cycle defined in the test rig DSP controller and presents a low sensitivity in execution time for the different modulation methods, independently of the coordinate system used to describe the space vector demanded to the modulator. Several modern modulation techniques were obtained with the proposed generalized algorithm by adjusting the modulation ratio δ in selected areas in the hexagonal space. Additionally, the proposed approach leads to a reduction in the computational burden of these modern modulation methods compared with the conventional implementations. The performance of the generalized algorithm has been verified in a VSI test rig, and the experimental results obtained with each of the tested modulation strategies are in complete agreement with the ones available in literature [16, 21, 33].

References

[1] V. T. Somasekhar, S. Srinivas, and K. Kumar: Effect of Zero-vector Placement in a Dual-inverter Fed Open-end Winding Induction Motor Drive With Alternate Sub-hexagonal Center PWM Switching Scheme, IEEE Transactions on Power Electronics, vol. 23, no. 3, pp. 1584-1591, May 2008.

[2] D. Casadei et al.: General modulation strategy for seven-phase inverters with independent control of multiple voltage space vectors, IEEE Transactions on Power Electronics, vol. 55, no. 5, pp.

1921-1932, May 2008.

[3] D. Dujic, G. Grandi, M. Jones, and E. Levi: A space vector PWM scheme for multifrequency output voltage generation with multiphase voltage-source inverters, IEEE Transactions on Industrial Electronics, vol. 55, no. 5, pp. 1943-1955, May 2008.

[4] J. Zubek, A. Abbondanti, and C. J. Norby: Pulsewidth modulated inverter motor drives with improved modulation, IEEE Transactions on Industry Applications, vol. 11, no. 6, pp. 695-703, Nov. 1975.

[5] M. A. Jabbar, A. M. Khambadkone, and Z. Yanfeng: Space-vector modulation in a two-phase induction motor drive for constant-power operation, IEEE Transactions on Power Electronics, vol. 51, no. 5, pp. 1081-1088, Oct 2004.

[6] L. Asiminoaei, P. Rodriguez, and F. Blaabjerg: Application of discontinuous PWM modulation in active power filters, IEEE Transactions on Power Electronics, vol. 23, no. 4, pp. 1692-1706, July 2008.

[7] J. H. Youm and B. H. Kwon: An effective software implementation of the space-vector modulation, IEEE Transactions on Power Electronics, vol. 46, no. 4, pp. 866-868, Aug 1999.

[8] L. Hao, X. Xiangning, and X. Yonghai: Study on the simplified algorithm of space vector PWM, in Power Electronics and Drive Systems, vol. 2, Singapore, Nov 2003, pp. 17-20.

[9] A. M. Hava and E. Un: Performance Analysis of Reduced Common-Mode Voltage PWM Methods and Comparison With Standard PWM Methods for Three-Phase Voltage-Source Inverters, IEEE Transactions on Power Electronics, vol. 24, no. 1, pp. 241-252, Jan 2009.

[10] G. Narayanan, V. T. Ranganathan, D. Zhao, H. K. Krishnamurthy, and R. Ayyanar: Space vector based hybrid PWM techniques for reduced current ripple, IEEE Transactions on Power Electronics, vol. 55, no. 4, pp. 1614-1627, Apr 2008.

[11] J. R. Wells, B. M. Nee, P. L. Chapman, and P. T. Krein: Selective harmonic control: a general problem formulation and selected solutions, IEEE Transactions on Power Electronics, vol. 20, no. 6, pp. 1337-1345, Nov 2005.

[12] A. M. Trzynadlowski, R. L. Kirlin, and S. F. Legowski: Space vector PWM technique with minimum switching losses and a variable pulse rate for VSI, IEEE Transactions on Power Electronics, vol. 44, no. 2, pp. 173-181, Apr 1997.

[13] Zheng Wang, K. T. Chau, and Chunhua Liu: Improvement of electromagnetic Compability of Motor Drives Using Chaotic PWM, IEEE Transactions on Magnetics, vol. 43, no. 6, pp. 2612-2614, June 2007.

[14] K. Zhou and D. Wang: Relationship between space-vector modulation and three-phase carrier-based PWM: a comprehensive analysis, IEEE Transactions on Power Electronics, vol. 49, no. 1, pp. 186-196, Feb 2002.

[15] J. M. D. Murphy and M. G. Egan: A Comparison of PWM Strategies for Inverter-fed Induction Motors, IEEE Transactions on Industry Applications, vol. 19, pp. 363-369, May 1983.

[16] A. M. Hava, R. J. Kerkman, and T. A. Lipo: Simple analytical and graphical methods for carrier-based PWM-VSI drives, IEEE Transactions on Power Electronics, vol. 14, no. 1, pp. 49-61, Jan 1999.

[17] M. A. Boost and P. D. Ziogas: State-of-the-art carrier PWM techniques: a critical evaluation, IEEE Transactions on Industry Applications, vol. 24, no. 2, pp. 271-280, Mar/Apr 1988.

[18] J. Holtz: Pulsewidth modulation-a survey, IEEE Transactions on Power Electronics, vol. 39, no. 5, pp. 410-420, Oct 1992.

[19] J. Holtz: Pulsewidth modulation for electronic power conversion, Proc. IEEE, vol. 82, no. 8, pp. 1194-1214, Aug. 1994.

[20] H. W. van der Broeck, H. C. Skudelny, and G. V. Stanke: Analysis and realization of a pulsewidth modulator based on voltage space vectors, IEEE Transactions on Industry Applications, vol. 24, no. 1, pp. 142-150, Jan/Feb 1988.

[21] O. Ojo: The generalized discontinuous PWM scheme for three-phase voltage source inverters, IEEE Transactions on Power Electronics, vol. 51, no. 6, pp. 1280-1289, Dec 2004.

[22] Z. Shu, J. Tang, Y. Guo, and J. Lian: An efficient SVPWM algorithm with low computational overhead for three-phase inverters, IEEE Transactions on Power Electronics, vol. 22, no. 5, pp. 1797-1805, Sep 2007.

[23] S. de Pablo, A. B. Ray, L. C. Herrero, and J. M. Ruiz: A simpler and faster method for SVM implementation, in Proceedings of Power Electronics and Applications, pp. 1-9, Sep 2007.

[24] J. Restrepo et al.: Direct power control of a dual converter operating as synchronous rectifier, IEEE Transactions on Power Electronics, vol. 26, no. 5, pp. 1410-1417, May 2011.

[25] G. Narayanan and V. T. Ranganathan: Triangle-comparison approach and space vector approach to pulsewidth modulation in inverter fed drives, Journal of the Indian Institute of Science, vol. 80, pp. 409-427, Sep/Oct 2000.

[26] H. Lu, W. Qu, X. Cheng, Y. Fang, and X. Zhang: A novel PWM technique with two-phase modulation, IEEE Transactions on Power Electronics, vol. 22, no. 6, pp. 2403-2409, Nov 2007.

[27] G. B. Kliman and A. B. Plunkett: Development of a modulation strategy for a PWM inverter drive, IEEE Transactions on Industry Applications, vol. 15, no. 1, pp. 72-79, Jan. 1979.

[28] V. Blasko: Analysis of a hybrid PWM based on modified space-vector and triangle-comparison methods, IEEE Transactions on Industry Applications, vol. 33, no. 3, pp. 756-764, May/Jun 1997.

[29] C. B. Jacobina, A. M. Nogueira Lima, E. R. C. da Silva, R. N. C. Alves, and P. F. Seixas: Digital scalar pulse-width modulation: a simple approach to introduce nonsinusoidal modulating waveforms, IEEE Transactions on Power Electronics, vol. 16, no. 3, pp. 351-359, May 2001.

[30] J. Restrepo, J. Aller, J. Viola, A. Bueno, and T. G. Habetler: Parallelogram Based Method for Space Vector Pulse Width Modulation, Rev. Fac. Ing. Univ. Antioquia, no. 52, pp. 161-171, Mar 2010.

[31] A. M. Hava, R. J. Kerkman, and T. A. Lipo: Carrier-based PWM-VSI overmodulation strategies: analysis, comparison, and design, IEEE Transactions on Power Electronics, vol. 13, no. 4, pp. 674-689, July 1998.

[32] A. M. Hava, R. J. Kerkman, and T. A. Lipo: A high-performance generalized discontinuous PWM algorithm, IEEE Transactions on Industry Applications, vol. 34, no. 5, pp. 1059-1071, Sep/Oct 1998.

[33] A. M. Hava, S. K. Sul, R. J. Kerkman, and T. A. Lipo: Dynamic overmodulation characteristics of triangle intersection PWM methods, IEEE Transactions on Industry Applications, vol. 35, no. 4, pp. 896-907, Jul/May 1999.

[34] D. W. Chung, J. S. Kim, and S. K. Sul: Unified voltage modulation technique for real-time three-phase power conversion, IEEE Transactions on Industry Applications, vol. 34, no. 2, pp. 374-380, Mar/Apr 1998.

The authors

Jose Alex Restrepo was born in Cali, Colombia, in 1964. He received the B.Sc. and M.Sc. degrees in electronics engineering from the Universidad Simon Bol›var, Caracas, Venezuela, in 1988 and 1991, respectively, and the Ph.D. degree from the University of Manchester Institute of Science and Technology, Manchester, U.K., in 1996. He is currently a Full Professor of electronics engineering in the Departamento de Electronica y Circuitos, Universidad Simon Bol›var. He has been a Visiting Professor at the School of

Electrical and Computer Engineering, Georgia Institute of Technology, Atlanta, in 2002 and 2010. His research interests include advanced control of electrical machines, artificial intelligence, power quality and digital signal processors applied to motion control.

Jose Manuel Aller was born in Caracas, Venezuela, in 1958. He received the Electrical Engineer degree from the Universidad Simón Bolívar, Caracas, in 1980, the M.Sc. in Electrical Engineering degree from the Universidad Central de Venezuela, Caracas, in 1982, and the Dr. in Industrial Engineering degree from the Universidad Politécnica de Madrid, Madrid, Spain, in 1993. He has been a Lecturer at the Universidad Simón Bolívar for 30 years, where he is currently a Full Time Professor in the Departamento de Conversión y Transporte de Energía teaching electrical machines and power electronics. He was the General Secretary of the Universidad Simón Bolívar from 2001 to 2005. He has been visiting professor at the Georgia Institute of Technology, Atlanta, USA, in 2000 and 2007. His research interests include space-vector applications, electrical machine control, power electronics and monitoring of electrical machines.

Alexander Bueno was born in Caracas, Venezuela in 1971. He received the Electrical Engineer degree and the M.Sc. in Electrical Engineering degree from the Universidad Simón Bolívar, Caracas, Venezuela, in 1993 and 1997, respectively. He has been a Lecturer at the Universidad Simón Bolívar for 16 years, where he is currently a Full Time Professor in the Departamento de Conversión y Transporte de Energía teaching electrical machines and power electronics. Currently, his research interests include space vector control applications, electrical machines, neural network estimators and power electronics.

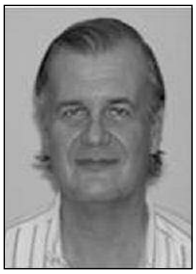

Víctor Manuel Guzmán was born in Zaragoza, Spain, in 1952. He received the Electronic Engineer degree from the Universidad Simón Bolívar, Caracas, Venezuela, in 1975, and the M.Sc. and Ph.D. degrees in Power Electronics and Systems from the University of Manchester Institute of Science and Technology (UMIST), Manchester, U.K, in 1978 and 1991, respectively. He started working at the Department of Electronics and Circuits, Universidad Simón Bolívar in 1975, and since 1993 he has been a Full Professor in the mentioned Department. His research interests include power electronics circuit design, device modeling, and renewable energy sources.

María Isabel Giménez was born in Caracas, Venezuela, in 1952. She received the Electronic Engineer degree from the Universidad Simón Bolívar, Caracas, Venezuela, in 1974, and the M.Sc. and Ph.D. degrees in Power Electronics and Systems from the University of Manchester Institute of Science and Technology (UMIST), Manchester, U.K, in 1978 and 1991, respectively. She started working at the Department of Electronics and Circuits, Universidad Simón Bolívar in 1974, and since 1992 she has been a Full Professor in the mentioned Department. Her research interests include circuit simulations, modulation algorithms and power electronics system design.